We are IntechOpen, the world's leading publisher of Open Access books Built by scientists, for scientists

4,800
Open access books available

122,000
International authors and editors

135M
Downloads

Our authors are among the

154
Countries delivered to

TOP 1%
most cited scientists

12.2%
Contributors from top 500 universities

CLARIVATE ANALYTICS BOOK CITATION INDEX INDEXED

WEB OF SCIENCE™

Selection of our books indexed in the Book Citation Index in Web of Science™ Core Collection (BKCI)

Interested in publishing with us?
Contact book.department@intechopen.com

Numbers displayed above are based on latest data collected.
For more information visit www.intechopen.com

4

Structure and Properties of Dislocations in Silicon

Manfred Reiche[1] and Martin Kittler[2]
[1]*Max Planck Institute of Microstructure Physics, Halle*
[2]*IHP microelectronics, Frankfurt (Oder)*
Germany

1. Introduction

Defects in crystalline materials modify locally the periodic order in a crystal structure. They characterize the real structure and modify numerous physical and mechanical properties of a crystal. Crystal defects are generally divided by their dimension: point defects are also known as zero-dimensional (0-D) defects, while dislocations are 1-D, twins and grain boundaries are 2-D, and precipitates are denoted as 3-D defects. Dislocations were implemented for the first time in the early 1900th to explain the elastic behavior of homogeneous, isotropic media. Based on Volterra´s "distorsioni" (Volterra, 1907), Love has introduced the term "dislocation" to describe a discontinuity of displacement in an elastic body (Love, 1927). The application of this term to denote a particular elementary type of deviation from the ideal crystal lattice structure was due to Orowan (1934), Polanyi (1934), and Taylor (1934a, 1934b).
A dislocation is characterized by a vector parallel to the dislocation line and a displacement or Burgers vector which is a certain finite increment $\mathbf{b}$ induced by the elastic displacement vector $\mathbf{u}$. The Burgers vector is equal to one of the lattice vectors in magnitude and direction and may be written as (Hirth & Lothe, 1982)

$$\oint du_i = \int \frac{\partial u_i}{\partial s} ds = -b_i \ . \tag{1}$$

The direction along the contour s is that of a right-hand screw relative to the chosen direction along the dislocation line ℓ, that is, relative to the unit vector $\mathbf{t}$ tangent to the dislocation line (Frank, 1951). The edge dislocation, introduced by Orowan (1934), Polanyi (1934), and Taylor (1934a, 1934b), is represented by the line ℓ along which the vectors $\mathbf{t}$ and $\mathbf{b}$ are perpendicular. If the vectors $\mathbf{t}$ and $\mathbf{b}$ are parallel, then the corresponding dislocation is called a screw dislocation (Burgers, 1939, 1940). In many materials, dislocations are found where the line direction and $\mathbf{b}$ are neither perpendicular nor parallel and these dislocations are called mixed dislocations, consisting of both edge and screw character.
In the elastic theory of isotropic media a dislocation is a line representing the boundary of the slipped region. Its strength is characterized by the displacement. The strain field around the dislocation is depicted as a cylinder. Among other things, the model explains the strain distribution around the dislocation, but cannot describe the strain in the center, i.e. in the core of the dislocation. Furthermore, the model does also not regard the influence of the

lattice periodicity of real crystals. Burgers & Burgers (1935) as well as Taylor (1934a, b), Polanyi (1934), and Kochendörfer (1938) already pointed out that a dislocation moves by skipping individual atoms via potential walls. A first phenomenological model considering a potential energy of displacement that reflects the lattice periodicity was proposed by Frenkel and Kontorova (see Dehlinger and Kochendörfer, 1940). The model was modified by Peierls (1940) and extended by Nabarro (1947). Here, the displacement of the crystal lattice and the associated stress are considered to be caused by a number of infinitesimal dislocations originally suggested by Eshelby (1949). For edge dislocations, the width, or core region, in the Peierls-Nabarro model is given by

$$2\xi = d/(1-\nu) \tag{2}$$

where d is the lattice plane distance and ν is the Poisson ratio. The introduction of the parameter ξ has the effect of removing the singularity at the origin of the dislocation that is present in model of Volterra (Hirth & Lothe, 1982). For screw dislocations the Peierls-Nabarro model assumes a stress component near the core which spreads out of the plane. This phenomenon anticipates the dissociation of a dislocation. The model also explains the motion of dislocations and results in the introduction of the Peierls energy, which represents the periodic displacement potential energy, as well as the Peierls stress required to overcome this potential barrier. The concept of kinks and jogs in dislocation lines is also a consequence of the model (Friedel, 1979). The Peierls-Nabarro model has been influential in the development of dislocation theory of more than 60 years. It was, for instance, modified to explain the dislocation motion (Hirth & Lothe, 1982), or to understand the structure of the dislocation core (Duesbery & Richardson, 1991; Bulatov & Cai, 2006).

Early investigations on semiconductor materials indicated the presence of electrically charged dislocations. It was already proved by Gallagher (1952) that plastic deformation of silicon and germanium increases their resistivity. Hall effect measurements suggested the introduction of acceptor-type levels in n-type Ge by deformation which was explained by negatively charged dislocation lines screened by a positive space charge region (Pearson et al., 1954). Based on these results and a remark of Shockley that dangling bonds in the core of an edge dislocation exist, Read (1954a,b) formulated a phenomenological theory of charged dislocations. He introduced the concept of dislocation electron levels, the occupation ratio of dislocation levels, and the radius of a Read cylinder surrounding each charged dislocation and screening the linear charge localized on it. Read (1954a,b) assumed that the dislocation states are represented by a single level or a one-dimensional band which is empty when the dislocation is in the neutral state. This assumption is applicable only at low temperatures (Labusch & Schröter, 1980). On the other hand, Schröter and Labusch (1969) argue that even at higher temperatures the dislocation band is half filled in the neutral state. Furthermore, dangling bonds does not exist in real dislocations. Numerous theoretical and experimental investigation particularly on dislocations in silicon refer to reconstructed dislocation cores. Therefore the electrical activity is related to defects on the dislocation core, such as kinks, jogs, and also by point defects bound to the core or in the elastic or electric field of the dislocation (Schröter & Cerva, 2002). While different types of dislocations are distinguished by different core defects their electrical activity is different (Alexander & Teichler, 1991). In addition, the concentration of point defects interacting with dislocations is doubtful even in the case of elemental semiconductors.

The present chapter reviews the current understanding about the structure and properties of dislocations in silicon and is based on earlier reviews given for instance by Bulatov et al. (1995), Alexander & Teichler (2000), Schröter & Cerva (2002), Spence (2007), and Kveder & Kittler (2008). All these papers demonstrate a substantial progress over the years but show also that a number of problems such as dislocation mobility, structure of the dislocation core, or electronic properties are not completely solved (George & Yip, 2001; Spence 2007). For instance, *ab-initio* computer simulations using different approaches result in a large number of models of the core structure of different dislocations which are not verified experimentally. The experimental data of dislocation motion can only be partially simulated by limiting the number of atoms, etc. (Bulatov & Cai, 2006). Another problem is the fundamental difference between theoretical calculations and experiment. While only individual dislocations are regarded in most of the calculations, a large number of dislocations is involved in experimental measurements such as plastic deformation. These measurements integrate not only over a number of dislocations but may also include data of different dislocation types and the interaction with a more or less unknown concentration of point defects. A further paragraph of this chapter is therefore dedicated to the preparation and characterization of only a small number of defined dislocations.

2. Structure of dislocations in silicon

Silicon crystallizes in the cubic diamond structure (space group Fd3m). The lattice constant is a = 0.543 nm. The glide plane is {111} and perfect dislocations have Burgers vectors of the type $\mathbf{b} = a/2\langle 110\rangle$. Hornstra (1958) has introduced two types of perfect dislocations in the diamond lattice: a pure screw dislocation and the so-called 60° dislocation, where the Burgers vector is inclined at an angle of 60° to the dislocation line. The diamond structure corresponds to two face-centered cubic (fcc) lattices displaced by $(1/4, 1/4, 1/4)$. Hence, atoms in both lattices do not have identical surroundings. Due to this fact, there are two distinct sets of {111} lattice planes; the closely spaced glide subset and the widely spaced shuffle subset (Hirth & Lothe, 1982). There is a long controversial discussion about the dominant dislocation type in the diamond structure. Early publications suggest the presence of dislocations in the shuffle set because movement through one repeat distance on a shuffle plane breaks one covalent bond per atomic length of dislocation (e.g. Seitz, 1952). The equivalent step on a glide plane involves the breaking of three bonds (Amelinckx, 1982). The idea of splitting or dissociation of perfect dislocations in the diamond structure has been commented for the first time by Shockley (1953) and was experimentally proved later on by electron microscopy. The introduction of the weak-beam method by Cockayne et al. (1969) has particularly shown that dislocations in silicon are in general dissociated and glide in this extended configuration. Both the screw and 60° dislocation belonging to the glide set can dissociate into pairs of partial dislocations bounding an intrinsic stacking fault ribbon (Ray & Cockayne, 1971; Gomez et al., 1975; Gomez & Hirsch, 1977). On the other hand, screw and 60° dislocations of the shuffle set can only dissociate into partials bounding an intrinsic stacking fault if there is a row of either vacancies or interstitials associated with one of the partials (Amelinckx, 1982). Most of the evidence indicates that the dislocations found in plastically deformed silicon belong to the glide set (Hirsch, 1985; Alexander, 1986; Duesbery & Joós, 1996).

For the 60° dislocation a 30° partial and a 90° partial dislocation are formed through dissociation, while the screw dislocation dissociates into two 30° partials (Gomez et al., 1974; Heggie and Jones, 1982). These is described by the dissociation reaction (Marklund, 1979)

$$\mathbf{b} \rightarrow \mathbf{b_1} + \mathbf{b_2}\,, \tag{3}$$

where in the case of a 60° dislocation

$$\mathbf{b} = \frac{a}{2}[011] \qquad \mathbf{b_1} = \frac{a}{6}[121] \qquad \mathbf{b_2} = \frac{a}{6}[\bar{1}11] \tag{4a}$$

and for a screw dislocation

$$\mathbf{b} = \frac{a}{2}[011] \qquad \mathbf{b_1} = \frac{a}{6}[121] \qquad \mathbf{b_2} = \frac{a}{6}[21\bar{1}] \tag{4b}$$

holds. The 30° as well as the 90° dislocations are of the Shockley type. The dissociation result as well in the formation of a stacking fault between both partial dislocations. The size of the stacking fault, i.e. the width of the splitting of the perfect dislocations d_0, depends in a stress free crystal on the stacking fault energy γ_{SF} and the repulsion force F of the partial dislocations

$$d_0 = \frac{F}{\gamma_{SF}} \tag{5}$$

The repulsion force is calculated using elastic constants given by the linear theory of elasticity resulting in (Amelinckx, 1982)

$$d_0 = \frac{Gb^2}{8\pi\gamma_{SF}} \cdot \frac{2-\nu}{1-\nu} \cdot \left(1 - \frac{2\nu}{2-\nu}\right) \cdot cos2\Theta \tag{6}$$

where G is the shear modulus, and Θ the angle between the dislocation line and the Burgers vector of the perfect dislocation. In a stressed crystal the two partials are exposed to additional forces which are in general different. Depending on the crystallographic orientation the external stress causes an increase or a decrease of d_0. Therefore the width of the splitting of a dislocation d_D by applying a resolved shear stress τ_s is given by (Wessel & Alexander, 1977)

$$d_D = \frac{d_0}{1 + \left[\not{f} - \frac{1-\alpha}{1+\alpha}\right] \cdot \frac{b\tau_s}{2\gamma_{SF}}} \tag{7}$$

with $\not{f}$ being a geometric factor and $\alpha = \mu_1/\mu_2$ as the ratio of mobilities μ_j of both partial dislocations.

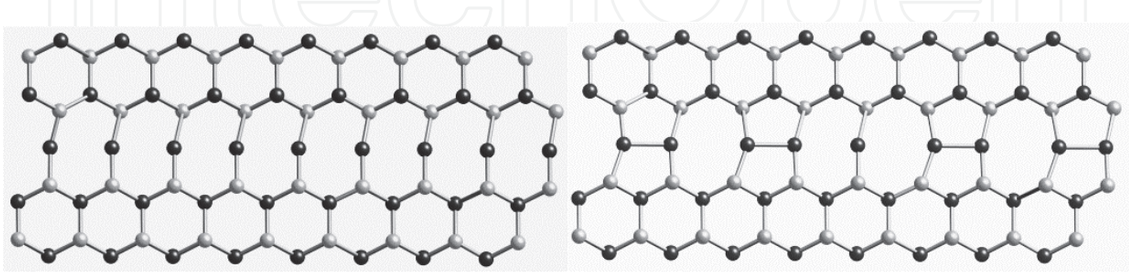

(a) (b)

Fig. 1. Models of the core structure of an unreconstructed (a) and a reconstructed 30° partial dislocation (b) according to Northrup et al. (1981) and Marklund (1983).

The initial models of perfect dislocations assumed dangling bonds in their core (Shockley, 1953; Hornstra, 1958). Experimental data, however, obtained mainly by electron paramagnetic resonance (EPR) spectroscopy refer to a low density of such dangling bonds (Alexander & Teichler, 2000). Dislocations of the glide set reconstruct by dissociation (Heggie & Jones, 1983; Marklund, 1983; Alexander, 1991), while dislocations of the shuffle set, which may exist at high applied shear stress, can stabilized by interaction with vacancies (Li et al. 2008). Different models of the core structure of partial dislocations have been suggested (figure 1, 2). The model of an unreconstructed 30° partial dislocation was presented and verified experimentally by high-resolution transmission electron microscopy (HRTEM) by Northrup et al. (1981). Models of the reconstructed 30° partial dislocation were proposed by Marklund (1983), Chelikowsky (1982), and Csányi et al. (2000). In this configuration, the dangling bonds are saturated after the pairs of neighbouring core atoms move closer together to form bonded dimers. The reconstruction breaks the translation symmetry and doubles the period along the dislocation line from b to 2b, where b is the magnitude of the Burgers vector. A defect appears at the boundary between two segments reconstructed in the opposite sense (so-called antiphase defect (Hirsch, 1979) or soliton (Heggie & Jones, 1983)).

The core reconstruction of the 90° partial dislocation was studied for more than 30 years. The driving force for core reconstruction is the same as for the 30° partial, that is the high energy of the unsaturated dangling bonds. A first model was proposed by Hirsch (1979). In this reconstruction there is a displacement that breaks the mirror symmetry normal to the dislocation line, enabling threefold coordinated atoms in the unreconstructed core to come together and bond. In this way two degenerate reconstructions exist. This core reconstruction is shown in figure 2a. The symmetry breaking displacement does not alter the translational symmetry along the dislocation line, which retains the same periodicity as the crystal (Bulatov et al., 2001). Another core reconstruction was proposed by Duesbery et al. (1991). In this structure the mirror symmetry is not broken and the atoms on either side of the dislocation line move towards each other so that each core atom has three nearest neighbours plus two more neighbours at a somewhat greater distance. This reconstruction is known as the quasi-fivefold reconstruction. Simulations, however, indicate that the quasi-fivefold configuration was higher in energy (Bigger et al., 1992). Benetto et al. (1997) proposed a new core reconstruction for the 90° partial dislocation with double the periodicity along the dislocation line (figure 2b). They found also that this reconstruction has a lower potential energy than the single period reconstruction. Further simulations,

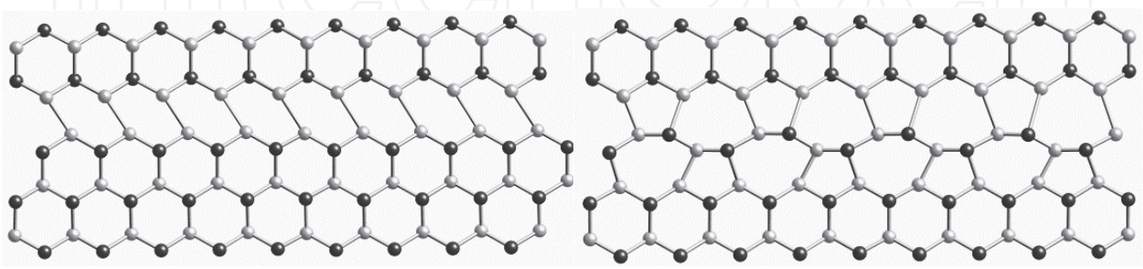

(a) (b)

Fig. 2. Models of the core structure of a single period (a) and a double period reconstruction of a 90° partial dislocation (b) according to Bulatov et al. (2001).

however, have shown that the energy differences between the single and double period structures are very close (Lehto & Öberg, 1998).

3. Electronic properties of dislocations in silicon

Dislocations interfere the translational symmetry of the crystal. As a consequence energy levels in the band gap result. First analyses were done by Read (1954a, b) who concerned with long-range screening and occupation statistics in the presence of the macroscopic band bending due to the dislocation. Based on early experiments of the plastic deformation of heavily doped p-type Ge single crystals (Gallagher, 1952; Pearson et al., 1954) Read concluded that only an acceptor level is introduced by edge dislocation. According to this model the dislocation is negatively charged. The line charge of the dislocation is screened by ionized donor atoms in a cylinder. Free electrons cannot penetrate this space charge cylinder and are scattered by specular reflection at its surface. For the position of the energy level of the neutral dislocation Read (1954a) obtained a value of 0.2 eV below the conduction band. The acceptor model of the dislocation states was not confirmed by measurements on p-type Ge and Si with lower doping levels (Schröter, 1969; Weber et al., 1968). It was concluded that dislocations can act as acceptors and as donors and consequently a partially filled band was attributed to the dislocation, in agreement with theoretical predictions (Schröter & Labusch, 1969). Veth and Lannoo (1984) combined the models of Read and Schröter & Labusch. They carried out a self-consistent calculation of the potential in the vicinity of the dislocation, point to an intraatomic Coulomb term *J*, and treat screeing in the dislocation core as dielectric perturbation. Outside the core, classical screeing by ionized dopant atoms or free carriers take place. The transition between the two screening mechanisms was analyzed. From this analysis follows a parameter-free formula for the total shift of the dislocation level E_e with respect to the edge of the undisturbed valence band

$$E_e = \frac{Jp}{\epsilon} + \frac{2e^2 p}{\epsilon a}\left[ln\left(\frac{R}{a}\right) - 0.616\right] \tag{8}$$

with p as the number of excess electrons per atom, ϵ the dielectric constant, *a* the distance between two core atoms, and R as the radius of the screening space-charge cylinder (Read cylinder), given by

$$R = (a \cdot \pi \cdot |N_D - N_A|)^{-1/2} \tag{9}$$

In Eq. (8) N_D and N_A are the concentrations of donors and acceptors, respectively. Veth and Lannoo (1984) pointed out that Eq. (8) is linear with p, which fits the experimental data with Read´s model and corresponds to the line charge model by Labusch & Schröter (1980). There are several problems that have to be solved by any model of the charged dislocation core. One is the electrostatic potential around a charged dislocation. Another is the mobility of the charges on the dislocation line.

Computer simulations result in a number of deep levels related to defects on the dislocation core (Alexander & Teichler, 1991). The energy levels depend strongly on the geometry of the defects. For instance, the structure and resulting energy levels of 30° partial dislocations were studied by Marklund (1979), Northrup et al. (1981), Chelikowsky (1982), and Csányi et al. (2000). Deep levels related to 60° or 90° partial dislocations were summarized by Alexander & Teichler, 1991). All the computer simulations clearly demonstrate that deep levels are caused by core bond reconstruction and reconstruction defects. Most of the

models, however, prefer reconstruction defects (antiphase defects, solitons) to explain the electronic properties of dislocations (Marklund, 1979; Heggie & Jones, 1983; Justo & Assali, 2001). Furthermore, electronic band gap calculations in combination with electron energy loss spectroscopy of dislocations in GaN revealed that impurities bonded to the dislocation core may induce electronic levels in the band gap (Bangert et al., 2004). On the other hand, the interaction of core defects with otherwise electronically active centers can also result in inactive complexes (Heggie et al., 1993; Jones et al., 1993).

Besides deep levels related to the dislocation core, shallow levels exist corresponding to more extended states, either states associated with stacking faults between two partial dislocations or states of electrons and holes trapped in the elastic deformation field of the dislocation. Calculations of energy levels related to stacking faults refer to the existence of shallow levels up to 0.1 eV above the valence band edge (Marklund, 1981; Mattheiss & Patel, 1981; Lodge et al., 1989). The shift of point defect levels relative to the silicon band edge may also be caused by the dislocation strain field. The response of the Si band structure to homogeneous elastic stresses has been investigated and is described by the deformation potential Ξ_{ij} (Bardeen & Shockley, 1950), which is written for the conduction band edge as (Keyes, 1960)

$$\Delta E_c = \sum_{i,j} \Xi_{ij} \cdot \varepsilon_{ij} \tag{10}$$

where ε_{ij} denotes the components of the strain tensor. Considering one minimum in the centre of the Brillouin zone and assuming an elastically isotropic material as an approximation, the shift of the conduction band minimum is given by the trace of the strain tensor and one component of the deformation potential tensor, Ξ_d (Schröter & Cerva, 2002):

$$\Delta E_c = \frac{b_e \cdot \Xi_d (1-2\nu)}{2\pi(1-\nu)} \cdot \frac{sin\Theta}{r} \tag{11}$$

In polar coordinate system Θ means the angle between $\mathbf{r}$ and b_e, the edge component of the Burgers vector. If Ξ_d is positive, the conduction band edge is lowered in the compressed region of an edge dislocation and increases in its tensile region. The behavior is reverse for negative values of Ξ_d. In addition, the strain field results also in an effective shift of the point defect level. If the strain-induced shift of the point defect level is described by the deformation potential Ξ_{pd}, one obtaines a position-depending shift $\Delta E_{c,pd}$ of the conduction band edge and point defect level (Schröter & Cerva, 2002)

$$\Delta E_{c,pd} = -\frac{b(\Xi_d - \Xi_{pd})(1-2\nu)}{2\pi(1-\nu)} \cdot \frac{sin\Theta}{r} \tag{12}$$

Analogous models for 60° and screw dislocations in p- and n-type elemental semiconductors (Si, Ge) have been proposed by Shikin & Shikina (1995).

The electrical activity of dislocations in silicon and germanium was studied by numerous methods where mostly plastic deformation was applied to produce defined dislocation arrangements (for instance, Schröter & Cerva, 2002; Alexander & Teichler, 2000). Hall effect measurement was primarily applied to verify the electrical activity of dislocations and to propose first models (Gallagher, 1952; Read, 1954a, b; Schröter & Labusch, 1969). Electron paramagnetic resonance (EPR) spectroscopy provides substantial information about the structure and, in combination with other techniques, electronic core defects (Kisielowski-

Kemmerich, 1990; Alexander, 1991; Alexander & Teichler, 1991, 2000). Plastic deformation introduces a variety of EPR-active defects in Si. Some of them denoted as Si-K1, Si-K2, Si-Y, and Si-R have been identified to be associated with the dislocation core, others, namely Si-K3, Si-K4, and Si-K5 with deformation-induced point defect clusters (Alexander & Teichler, 1991). Si-K6 and Si-K7 are ascribed to impurity atoms in the dislocation core. It was concluded that all EPR active centers attributed to dislocations belong to vacancies introduced into the core of the 30° partials forming screw dislocations. There is hitherto no satisfying explanation, why paramagnetic centers are not observable for 60° dislocations (and therefore 90° partials). EPR requires defined charge states of defects which can be different for 60° and screw dislocations.

Properties of deep levels generated by lattice defects are also investigated by deep level transient spectroscopy (DLTS) introduced by Lang (1974). The method probes changes of the capacity of the space charge region of a diode caused by reloading of deep levels. For point defects, emission and capture rate are linearly dependent on the occupation ratio of the defect level so that capacitance transients are exponentially dependent on time during capture and emission. The analysis of the DLTS-line variations with correlation frequency and filling pulse duration is then straightforward and yields the level of the defect (ionization enthalpy and entropy, its electron or hole capture cross section, and its concentration (Schröder & Cerva, 2002)). For dislocations, line charge fluctuations modify the electron emission resulting in a non-exponential transient and gives rise to a broadening of the corresponding DLTS line (Figielski, 1990). Some important features such as the C-line in n-type silicon, the F-line in p-type Si as well as B- and D-line in plastically deformed Si were analyzed in detail (for a review see e.g. Schröter & Cerva, 2002). The interaction of dislocations especially with metal impurities was also intensively studied with DLTS (Seibt et al., 2009a).

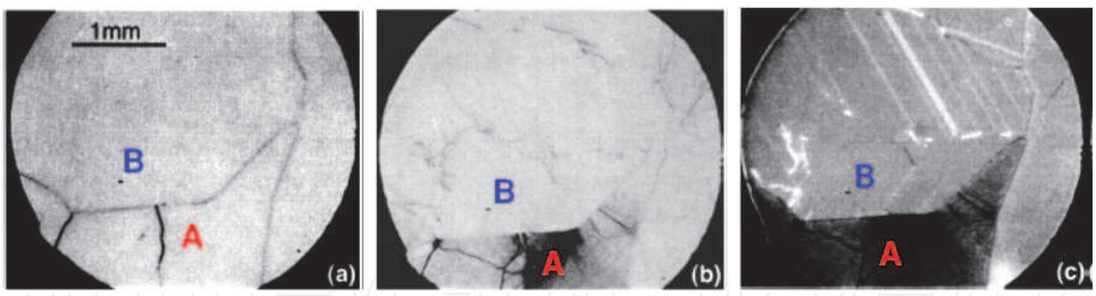

Fig. 3. Temperature dependence of the EBIC contrast of defects in multi-crystalline silicon. Measurements at 300K (a), 80K (b), and 30K (c).

Several techniques have been applied to analyze with spatial resolution the recombination activity of dislocations such as scanning deep level transient spectroscopy (SDLTS, Breitenstein & Wosinski, 1983), photoluminescence, light beam induced current (LBIC), and electron beam induced current (EBIC). EBIC and LBIC are unique among the electrical characterization methods with respect to a spatial resolution, sufficient to measure individual dislocations. In EBIC, for instance, the variation of the current at a Schottky contact resulting from excess electrons and holes generated locally by the electron beam is measured, when the specimen area of interest is scanned. The values of the current at the dislocation I_{dis} and away from it, I_0, are used to define the contrast $C_{dis} = (I_0-I_{dis})/I_0$ of single dislocations. The measurement involves the dependence of C_{dis} on the temperature and the

beam current of the electron probe. The temperature dependence of the defect contrast, $C_{dis}(T)$, is illustrated in figure 3 for different defects (intra-grain dislocations, grain boundaries, etc.) in multi-crystalline silicon. Furthermore, C_{dis} is proportional to the recombination rate of minority carriers at a dislocation. A theoretical description was derived by Donolato (1979, 1983) and Pasemann (1981). Numerous experimental investigations showed that dislocations in different Si materials often exhibit very different EBIC contrast behavior $C_{dis}(T)$ which is caused by different concentrations of deep intrinsic core defects and impurities. Different models were presented to explain the contrast behavior (Schröter and Cerva, 2002). A quantitative explanation of the experimental results was proposed by Kveder et al. (2001) which differs from earlier model (Wilshaw & Booker, 1985) by including electronic transitions between one-dimensional bands and deep localized states due to overlapping of their wave functions. Taking these transitions into account the dislocation recombination activity is properly described.

In 1976, Drozdov et al. (1976) proved lines in the photoluminescence spectra of deformed n- and p-type Si associated with dislocations. The lines are denoted as D1 – D4 (figure 4). The maximum position of the lines were measured at T = 4.2K as D1 = 0.812 eV, D2 = 0.875 eV, D3 = 0.934 eV, and D4 = 1.000 eV. The relative intensity of D1 to D4 depend on the dislocation density and distribution and can vary in different samples. The polarization of the D-lines emission and their response to uniaxial stress has been utilized to establish their relations to dislocations. Lines D1 and D2, on the one hand, and lines D3 and D4, on the other, show similar shifts by applying uniaxial stress and therefore have been grouped as pairs (Drozdov et al. 1977; Sauer et al., 1985). Polarization measurements were carried out to determine the electric field vector $\mathfrak{E}$ of the luminescent light. Using three different registration directions ($[21\bar{1}]$, $[1\bar{1}1]$, $[011]$), the $\mathfrak{E}$ vector within the primary slip plane, along $[1\bar{1}1]$, with a polarization of about 30% was found for D1/D2 (Weber, 1994). D3 and D4 exhibit an $\mathfrak{E}$ vector within the primary glide plane roughly along [011], i.e. along to the main Burgers vector, and with a polarization of about 20%. These findings strongly point to the dislocations as radiative centres for D3/D4. For D1/D2 the situation is more complex. The energy positions of D3 and D4 depend on the distance between partial dislocations suggesting that both originate from recombination processes at straight segments of 60° dislocations (Sauer et al., 1986, 1994). In addition, photoluminescence measurements on

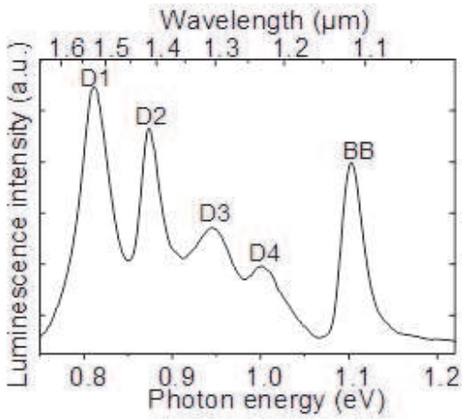

Fig. 4. Photoluminescence spectrum of dislocated silicon recorded at 80K. The spectrum shows the presence of dislocation-induced D-bands (D1 – D4) besides the band-band luminescence (BB).

dislocations in epitaxially grown SiGe layers refer to D3 as a phonon assisted replica of D4 (Weber & Alonso, 1990).
The origin of the D1 and D2 lines is still not understood. There are investigations referring that both lines are related to impurity atoms in the dislocation core (Higgs et al., 1993), dislocation jogs (Watson et al., 1998), or segments of dislocations (Lomer dislocations) appearing due to dislocation reactions, multi-vacancy and/or self-interstitial clusters trapped in the core (Jones et al., 2000).

4. Grain boundaries

Crystallization and recrystallization are typical processes to produce multi-crystalline silicon as the mostly applied material in solar cell manufacture. Multi-crystalline silicon, or in general polycrystalline materials, consists of numerous (single crystalline) grains with different crystallographic orientations separated by grain boundaries. The geometry of a grain boundary is macroscopically characterized by five degrees of freedom: three angles define the crystallographic orientation of both crystals with respect to each other, while two parameters describe the inclination of the grain boundary plane. To fully characterize the boundary geometry on a microscopic level, three additional parameters are required to define the atomic-scale relative translation of the two grains. Depending on the misorientation, grain boundaries are of the tilt type, when the rotation axis lies in the boundary plane, or of the twist type, when the rotation axis is normal to the boundary plane. A general grain boundary may have tilt and twist components.
Based on previous consideration of Burgers, Bragg, and Frank (see Amelinckx, 1982), first models of grain boundaries have been proposed by Shockley & Read (1949), Read & Shockley (1950), van der Merwe (1949), and Cottrell (1953). Besides a classification into tilt and twist boundaries, grain boundaries may be divided by their angle of misorientation Θ_{GB} into low-angle ($\Theta_{GB} < 5°$) and large-angle grain boundaries. More comprehensive definitions distinguish between singular, vicinal or general interfaces (Baluffi & Sutton, 1996), or between general (or random) and special grain boundaries (Chadwick & Smith, 1976). Special grain boundaries exhibit a periodic structure, while general grain boundaries show no appearent periodicity.
Numerous investigations have been carried out about the structure of grain boundaries in silicon. From these investigations it is concluded that (Seager, 1985):

1. Silicon grain boundaries are primarily composed of regular defects: perfect dislocations, partial dislocations, and stacking faults. There are no evidences for distinct amorphous phases at the grain boundary. This is true for all silicon materials grown by different techniques.
2. Low-angle ($\Theta_{GB} < 5°$) tilt and twist boundaries are not composed of regular arrays of perfect dislocations. Instead, several types of dislocations are present in the same boundary; some may be dissociated into partial dislocations forming a stacking fault in between. Most of these low-angle grain boundaries are reconstructed such that no dangling bonds remain.
3. Large-angle grain boundaries are usually composed of distinct facets. These facets with lengths of one or more nanometers are subsections of the boundaries where bonding rearrangements have occurred that are of a few known low-energy configurations. These configurations can usually be predicted using the concepts of the coincidence site lattice (CSL) theory (Gleiter & Chalmers, 1972; Chadwick & Smith, 1976; Sutton &

Baluffi, 1995). The arrangement of these facets is not always a simple, repetitive one and the average boundary interface angle can actually vary substantially over macroscopic distances.

4. Even simple first-order twin boundaries can display this irregular faceted structure at their interfaces. Dislocations frequently terminate at coherent twin boundaries, and the resulting intersection points disturb the atomic arrangements on the boundary plane.

The interaction of intragranular dislocations with grain boundaries is an important issue because grain boundaries are effective obstacles to dislocation motion. Dislocations coming upon a boundary generally do not have the same Burgers vector and slip plane to glide into the next grain. Most commonly, the elastic interaction between dislocations and grain boundaries is repulsive and consequently the dislocations pile up at the boundary. Dislocations, however, may also transmitted directly across the grain boundary if the slip planes on both sides intersect along a line that lies in the boundary plane. For pure screw dislocations, the Burgers vector remains unchanged. In contrast, the transmission of dislocations with an edge component requires the formation of a residual grain boundary dislocation with a Burgers vector equal to the difference of the Burgers vectors of the incoming and outgoing lattice dislocations. A dislocation may alternatively be absorbed by the boundary without emission of a dislocation in the adjacent grain. In this case, the lattice dislocation fully dissociates.

Another important issue related to grain boundaries is the diffusion of impurities. It is generally known that diffusion at grain boundaries is orders of magnitude faster compared to volume diffusion, and it plays a major role in processes that involve material transport, such as recrystallization, grain growth, grain boundary segregation, etc. Based on previous analyses, Queisser et al. (1961) measured the phosphorous diffusion on a particular grain boundary suggesting an enrichment of phosphorous near the boundary dislocations. More recent investigations support the enhanced diffusion at grain boundaries but measurements of the activation energy are quite different (Schimpf et al. 1994). Values of the activation energy ranging from 1.4 eV to 2.9 eV were reported indicating the effect of the grain boundary structure as well as the interaction with other impurities segregated at the boundary on the diffusion. There is a number of other investigations dealing with the diffusion of different elements into polycrystalline silicon. All these investigations show a different behavior for various elements. For instance, an enhanced diffusion was proved for boron and titanium (Corcoran & King, 1990), while the diffusion of Al is suppressed. Other elements tend to diffuse out (Salman et al., 2007).

In order to overcome the difficulties arising from the analyses of polycrystalline materials specific grain boundaries were of growing interest to study their structure and properties (for instance, Bourret & Bacmann, 1987; Thibault-Desseaux et al., 1989). The realization of the so-called bicrystals requires, however, a Czochralski growth process allowing only the formation of specific grain boundaries such as Σ = 9(122), Σ = 13(510), and Σ = 25(710) (Aubert & Bacmann, 1987).

A first model of the electrical activity of grain boundaries in Ge was proposed by Taylor et al. (1952). Based on measurements they concluded that the grain boundary acts as a potential barrier due to surface states. The center zone with a high density of states (assumed as broken bonds) and a space charge on either side represents a double Schottky barrier. The current across the grain boundary, I, is then given by

$$I = e\mu[(n_B - n_A) \cdot exp(\mp eV_{AB}/kT)]/[1 - exp(\mp eV_{AB}/kT)] \,, \tag{13}$$

where μ is the carrier mobility, E is the electric field at the top of the barrier, n_B the carrier density at the barrier top, n_A the carrier density on the bottom of the barrier, and V_{AB} the voltage measured across the barrier. The negative and positive signs are taken for electron current and hole current, respectively. Using the Richardson equation for thermoionic emission, Mueller (1961) write the zero-bias conductance G_0 of a grain boundary as

$$G_0 = (1 - \frac{\gamma}{2}) \cdot (e^2 N_c \overline{v}/4kT^2) \cdot e^{c/k} \cdot T \cdot e^{-\phi_0/kT} , \tag{14}$$

with γ the capture rate, e the electron charge, $\overline{v}$ the average thermal velocity, N_c the effective number of states, and ϕ_0 the barrier height at equilibrium. The model of Taylor et al. (1952) was developed further by Mataré (1984) and was successfully applied to interpret the electronic properties of grain boundaries in bicrystals (Broniatowski, 1985; Bourgoin et al. 1987). Seager (1985) proposed another model by integrating tunneling and thermoionic emission currents resulting in

$$G_0 = \frac{eA^*T}{k} \cdot \left\{ \frac{1}{kT} \int_0^{\phi_0} \frac{exp\left[\left(\frac{2}{E_0}\right)\left[[\phi_0(\phi_0 - E)]^{\frac{1}{2}} - E \cdot ln\left(\frac{\left(\phi_0^{\frac{1}{2}} + (\phi_0 - E)^{\frac{1}{2}}\right)}{E^{\frac{1}{2}}}\right)\right]\right]}{1 + exp[(E+\varsigma)/kT)]} dE + exp\left(\frac{-(\phi_0+\varsigma)}{kT}\right) \right\} \tag{15}$$

with A* as an effective Richardson constant, $\zeta = E_C - E_F$, $E_0 = (\hbar^2 e^2 N_d / 4 m_t \epsilon \epsilon_0)$, N_d the dopant concentration, and m_t as the tunneling mass. The second term in brackets of Eq. (15) is the standard thermoionic emission, while the first term describes the thermoionic field emission contributions to G_0.

If a dc bias is applied to the grain boundary, the band diagram is modified. Using simplifying assumptions (pinning of the Fermi level at the grain boundary, Mueller, 1961), the energy density of grain boundary states with respect to the applied voltage is given by Seager and Pike (1979) as

$$\overline{N}_T(E) = \left(\frac{\epsilon \epsilon_0 N_d}{2e^2}\right)^{1/2} \cdot \left[\phi_B^{-1/2} + \left(1 + \frac{e}{\phi_B'}\right)(\phi_B + eV)^{-1/2}\right] \tag{16}$$

for eV > kT. In Eq. (16) $\phi_B' = \partial \phi_B / \partial eV$ and ϕ_B is the barrier height given by

$$\phi_B = \phi_0 - kTln(eJ/G_0 kT) \tag{17}$$

Models describing especially the minority carrier transport and recombination processes on grain boundaries under optical illumination were presented, for instance, by Fossum & Sundaresan (1982) and Joshi (1987). Assuming a Gaussian distribution of interface states (other distributions were also discussed, see Joshi, 1987), the electron *n(0)* and hole concentrations *p(0)* at the grain boundary are obtained as

$$n(0) = N_d \cdot \exp(e\phi_B/kT) \tag{18}$$

and

$$p(0) = \frac{n_i^2}{N_d} \exp\left(\frac{\Delta E_F}{kT}\right) exp\left(\frac{e\phi_B}{kT}\right) \tag{19}$$

where n_i is the intrinsic carrier concentration and ΔE_F the separation of the quasi-Fermi levels at the grain boundary. ΔE_F is a function of the illumination level. Using the Shockley-Read-Hall theory, Joshi (1987) calculated the steady-state recombination current density at a grain boundary assuming a single interface energy level in the energy gap exists:

$$J_r(0) = e\sigma_n\sigma_c\overline{v}n_i^2[exp(\Delta E_F/kT) - 1] \cdot \int_{E_v(0)}^{E_c(0)} \frac{n_{gs}(E)}{\sigma_n n(0)+\sigma_n n_i\beta+\sigma_c p(0)+\sigma_c n_i\beta^{-1}}\, dE, \qquad (20)$$

where σ_c and σ_n are the Coulomb and neutral capture cross-sections for a recombination center, respectively, n_{gs} the energy distribution of the states and $\beta = \exp[(E\text{-}E_i)/kT]$, where E_i means the energy position of the mean value of the interface states distribution.

The increasing importance of multi-crystalline silicon in the production of solar cells results in a huge number of publications related to the analyses of grain boundaries. The analyses of trap levels on model grain boundaries were extensively investigated by Broniatowski (1985). Numerous measurements on individual grain boundaries in multi-crystalline silicon were presented. Recent results about the electrical activity of grain boundaries obtained by EBIC methods were published, for instance, by Chen et al. (2010), Sekiguchi et al. (2011), or Pandelov et al. (2002). These papers refer to numerous others published previously. Caused by the high local resolution EBIC methods were also utilized to study the segregation of dopands or metallic impurities on grain boundaries (e.g. Seibt et al., 2009). The passivation of interface states on grain boundaries by hydrogen was studied as well (Rinio et al. 2006; Chen et al., 2005).

Furthermore, luminescence-based techniques are widely applied in the characterization of grain boundaries in solar cell materials. Cathodoluminescence (Vernon-Parry et al., 2005) and photoluminescence (Mchedlidze et al., 2010; Dreckschmidt & Möller, 2011) are useful tools to characterize defects at grain boundaries and different multi-crystalline bulk and thin film materials. The high sensitivity of the band-to-band emission of silicon to recombination activity (Würfel, 1982) results in the development of micro-photoluminescence spectroscopy used to study individual defects as well as to characterize the quality of whole solar cell wafers. The method allows the characterization of impurities (metal precipitates) and their effect on the recombination behavior of extended defects (Gundel et al. 2009, 2010). Recently, the D-lines appearing in the photoluminescence spectrum of dislocated silicon were used as well. First results using photoluminescence (Schmid, 2011) and cathodoluminescence were reported (Lee et al., 2009; Sekiguchi et al. 2010). Another approach to study electrically active defects in multicrystalline materials is the so-called dark lock-in thermography (DLIT, Breitenstein et al., 2010).

5. Characterization of individual dislocations

A fundamental problem in studying dislocations is the realization of defined arrangements of these defects. Some of the methods need a higher concentration of the defects to attain the detection limit (such as EPR). In contrast, other methods, as electron microscopy, require only a few or individual dislocations to obtain reasonable results. The dominant method to produce defined dislocation arrangements is plastic deformation. Plastic deformation, however, result also in a large number of point defects and defect reactions making it sometimes difficult to interpret experimental data (Alexander et al., 1983; Alexander & Teichler, 1991). In order to avoid interactions between dislocations or between dislocations and other defects, methods are required allowing the realization and analyses of only a few

dislocations or, in the ideal case, of an individual dislocation. First attempts can be traced back into the 1970th. Eremenko et al. (see Shikin & Shikina, 1995) measured the current-voltage characteristics of a 60° dislocation. Similar experiments were also done by Milshtein (1979) a few years later. Their measurements demonstrated a diode behavior of the dislocation. The dislocation was assumed to pass the whole specimen and metallic tips were used as contacts which, however, were singnificantly larger than the dislocation diameter. Another approach to realize defined dislocation arrangements was the application of silicon and germanium bicrystals (Thibault-Desseaux et al., 1989). As pointed out before, only specific orientations of grain boundaries are viable by the Czochralski growth process. Another method to realize defined dislocation arrangements in a reproducible way is semiconductor wafer direct bonding. For wafer bonding commercially available wafers are used making it possible to realize any grain boundary. Especially small-angle grain boundaries having rotation angles below 1° are of interest allowing to separate dislocations by a few hundred nanometers. Such distances are large enough to analyze only a small number or individual dislocations.

The principle of semiconductor wafer direct bonding originally developed to produce silicon on insulator (SOI) substrates and three-dimensional micro-electromechanical systems (MEMS) was comprehensively described elsewhere (Tong & Gösele, 1998). If the native oxide is removed from the wafers, two Si surfaces are brought into contact (hydrophobic wafer bonding). A subsequent annealing transforms the original adhesion forces into Si-Si bonds via the interface. Crystal defects (dislocations) are generated forming a two-dimensional network (or grain boundary) in order to match both crystal lattices. The structure of the dislocation network depends on the surface orientation of both wafers. Screw dislocation networks, networks dominated by 60°, and interactions between both types of networks were realized and studied in detail (for instance, Reiche (2008)). The mesh size of the network or, the dislocation distance, is reproducibly adjusted by controlling the tilt and twist misorientation angles which can be calculated using Frank´s formula (Amelinckx, 1982). Dislocation distances of more than 100 nm are obtained by using misorientation angles below 0.1°. Note that misorientation angles down to 0.005° were realized using aligned wafer bonding processes (Wilhelm et al., 2008).

Properties of dislocation networks formed by semiconductor wafer direct bonding were described in numerous publications (for reviews see, e.g. Kittler et al., 2007; Kittler & Reiche, 2009). The dislocation networks may be considered as model structures resulting in a lot of new information about the structure and properties of dislocations. The electrical properties of bonded hydrophobic silicon wafers were studied for the first time by Bengtsson et al. (1992) using capacitance-voltage measurements. More recent EBIC analyses proved barrier heights generally smaller than 100 meV for different types of bonded hydrophobic wafers (Kittler & Reiche, 2009). The concentration of deep levels along the interface was determined to be a few 10^5 per cm.

The luminescence properties of dislocation networks were also studied. Figure 5a shows the luminescence spectra of different bonded samples. The spectra are obtained from samples having different misorientation. Detailed photoluminescence and cathodoluminescence measurements provide direct evidence that the wavelength of light emitted from the dislocation network could be tailored to some extent by misorientation of the wafers during the bonding procedure. D1 or D3 lines have the largest intensity in the spectra due to the variation of the twist angle from 8.2° to 9°. Thus the luminescence spectrum can be tailored

by the misorientation angles in a controlled manner and the dominance of either D1 or D3 radiation can be attained. Further investigations refer that screw dislocations dominantly effect the intensity of the D1 line. The photoluminescence spectra of three different dislocation networks are presented in figure 5b. The corresponding electron microscope images are shown in figure 5c. The dislocation network DN#1 is dominated by 60° dislocations running in the image parallel with a distance in between of about 30 nm. The network of the 60° dislocations is superposed by an additional network of screw dislocations having distances of more than 2 µm (not shown in the image). The other networks in figure 5c (DN#2, DN#3) are characterized by more or less hexagonal meshes caused by the interaction of two networks of 60° dislocations and screw dislocations, both with nearly the same dislocation distances therein. The photoluminescence spectra recorded at low temperature (80K) and room temperature show the presence of the D1-line around

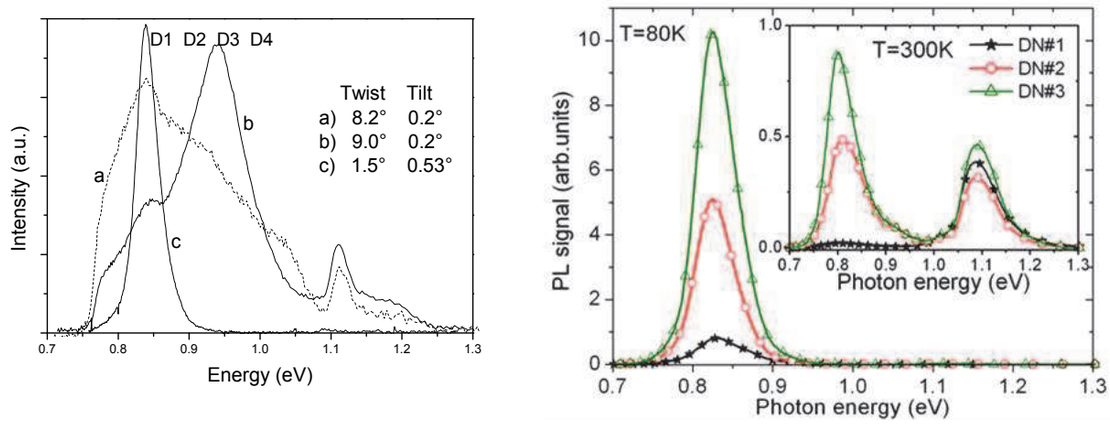

(a) (b)

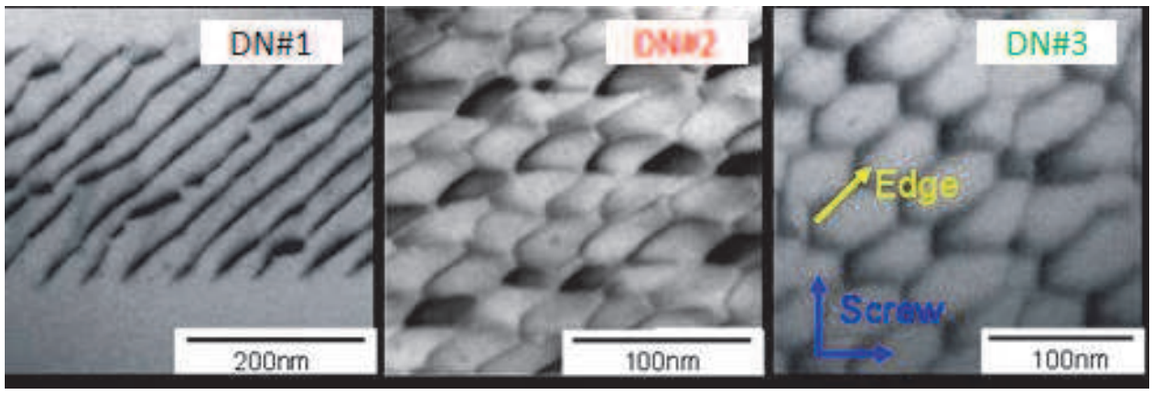

(c)

Fig. 5. The impact of the misorientation and dislocation structure on the luminescence spectra of dislocation networks. (a) The effect of misorientation (tilt and twist components). Cathodoluminescence spectra recorded at 80K. Photoluminescence spectra measured at 80K and room temperature (b) of three dislocation networks shown in (c).

(figure 5b). The spectra clearly prove the different intensity behavior depending on the dislocation structure and distance of the screw dislocations. The intensity of the D1-line is lowest in the spectrum of sample DN#1, characterized by the largest distance of screw dislocations, and increases as the distance of the screw dislocations decreases. The distance of screw dislocations in these particular samples is 15 nm (DN#2) and 32 nm (DN#3). Note that significant intensities of the D1-line are measured for DN#2 and DN#3 which are considerably stronger than that of the band-to-band-luminescence even at room temperature. According to these results it is suggested that radiative recombination is mainly caused by screw dislocations while 60° dislocations attribute preferentially to the non-radiative recombination.

A combination of wafer bonding with preparation methods to separate individual dislocations or a small number of dislocations allows the measurement of their electronic properties by elimination of interactions in between. As shown before, twist angles between two bonded Si wafers below 0.1° result in dislocation distances of more than 100 nm. Using photolithography and etching techniques, individual dislocations can be separated and measured. Typical structures applied were diodes and metal-oxide-semiconductor field-effect transistors (MOSFETs) (Reiche et al. 2010, 2011). The presented data clearly showed an indirect behavior of the drain current on the number of dislocations in the channel. The fact that the highest current is obtained if only a few dislocations are present allows the conclusion that electrically active centers in the dislocation core of the straight dislocation segments are responsible for the electron transport while dislocation nodes and dislocation segments oriented orthogonal to the channel direction act as “scattering centers” and reduce the carrier transport.

The single-electron tunneling on dislocations was recently studied by Ishikawa et al. (2006) on nMOSFETs prepared on dislocation networks produced by wafer bonding of SOI wafers. Measurements were done using a back gate contact (oxide thickness 400nm). Low-temperature measurements (T=15K) proved oscillations in the drain current – gate voltage curves indicating single-electron tunneling (Coulomb blockade oscillations). The lateral size of the Coulomb islands was estimated to be about 20 nm which agreed with the dislocation distance. From this Ishikawa et al. (2006) concluded that Coulomb islands are related to the dislocation nodes in the screw dislocation network. Very recent measurements at T = 4K by the authors proved also the existence of Coulomb blockade oscillations. Using nMOSFETs and applying a front side gate contact (gate oxide thickness 6 nm) lateral sizes of the Coulomb island of about 6 nm were extracted which do not correspond to dislocation nodes. Furthermore, a different behavior is observed for screw and mixed dislocations resulting from the reaction of screw and 60° dislocations. The single-electron tunneling was proved for one set (screw dislocations), while the other shows a more two-dimensional characteristics indicated by a staircase structure.

6. Acknowledgment

We would like to thank T. Arguirov, A. Hähnel, T. Mchedlidze, R. Scholz, W. Seifert, and O. Vyvenko for supporting this work. Parts of this work were financially supported by the German Federal Ministry of Education and Research in the framework of the SiliconLight project (contract no. 13N9734) and the SiGe-TE project (contract no. 03X3541B).

7. References

Alexander, H. (1986). Dislocations in Covalent Crystals, in: *Dislocation in Solids*, Vol. 7, F.R.N. Nabarro, pp. 113-234, North-Holland, Amsterdam

Alexander, H. (1991). Dislocations in Semiconductors, in: *Polycrystalline Semiconductors II*, J.H. Werner and H.P. Strunk, Springer Proc. In Physics, Vol. 54, Springer, Berlin, pp. 2-12

Alexander, H. & Teichler, H. (1991). Dislocations, in: *Materials Science and Technology*, *Vol. 4. Electronic Structure and Properties of Semiconductor*, W. Schröter, VCH, Weinheim, pp. 249-319

Alexander, H. & Teichler, H. (2000). Dislocations, in: *Handbook of Semiconductor Technology*, K.A: Jackson and W. Schröter, Wiley-VCH, Weinheim, pp. 291-376

Alexander, H., Kisielowski-Kemmerich, C., and Weber, E.R. (1983). Investigations of Well Defined Dislocations in Silicon, *Physica B,* Vol. 116, pp. 583-593

Amelinckx, S. (1982). Dislocations in Particular Structures, in: *Dislocation in Solids*, Vol. 2, F.R.N. Nabarro, pp. 67-460, North-Holland, Amsterdam

Aubert, J.J. & Bacmann, J.J. (1987). Czochralski Growth of Silicon Bicrystals, *Revue Phys. Appl*., Vol. 22, No. 7, pp. 515-518

Baluffi, R.W. & Sutton, A.P. (1996). Why Should We Interested in the Atomic Structure of Interfaces?, *Mat. Sci. Forum*, Vol. 207-209, pp. 1-12

Bangert, U., Harvey, A.J., Jones, E., Fall, C.J., Blumenau, A.T., Briddon, R., Schreck, M., and Hörmann, F. (2004). Dislocation-Induced Electronic States and Point Defect Atmospheres Evidenced by Electron Energy Loss Imaging, *New J. Phys*., Vol. 6, pp. 184-189

Bardeen, J. & Shockley, W. (1950). Deformation Potentials and Mobilities in Non-Polar Crystals, Phys. Rev., Vol. 80, No. 1, pp. 72-80

Benetto, J., Nunes, R.W., and Vanderbilt, D. (1997). Period-Double Structure for the 90° Partial Dislocation in Silicon, *Phys. Rev. Lett*., Vol. 79, No. 2, pp. 245-248

Bengtsson, S., Andersson, G.I., Andersson, M.O., and Engström, O. (1992). The Bonded Unipolar Silicon-Silicon Junction*, J. Appl. Phys*., Vol. 72, No. 1, pp. 124-140

Bigger, J.R.K., McInnes, D.A., Sutton, A.P., Payne, M.C., Stich, I., King-Smith, R.D., Bird, D.M., and Clarke, L.J. (1992). Atomic and Electronic Structures of the 90° Partial Dislocation in Silicon, *Phys. Rev. Lett.,* Vol. 69, No. 15, pp. 2224-2227

Bourgoin, J.C., Mauger, A., and Lannoo, M. (1987). Electronic Properties of Grain Boundaries in Semiconductors, *Revue Phys. Appl*., Vol. 22, No. 7, pp. 579-583

Bourret, A. & Bacmann, J.J. (1987). Atomic Structure of Grain Boundaries in Semiconductors, *Revue Phys. Appl*., Vol. 22, No. 7, pp. 563-568

Breitenstein, O. & Wosinski, T. (1983). Scanning-DLTS Investigation of the EL 2 Level in Plastically Deformed GaAs, *Phys. Stat. Sol.* (a), Vol. 77, K107-K110

Breitenstein, O., Bauer, J., Altermatt, P.P., and Ramspeck, K. (2010). Influence of Defects on Solar Cell Characteristics, *Solid State Phenom*., Vol. 156-158, pp. 1-10

Broniatowski, A. (1985). Electronic States at Grain Bounaries in Semiconductors, in: *Polycrystalline Semiconductors, Physical Properties and Applications*, G. Harbecke, pp. 95-117, Springer, Berlin

Bulatov, V.V., Yip, S., and Argon, A.S. (1995). Atomic Modes of Dislocation Mobility in Silicon, *Phil. Mag*. A, Vol. 72, No. 2, pp. 453-496

Bulatov, V.V., Justo, J.F., Cai, W., Yip, S., Argon, A.S., Lenosky, T., de Koning, M., and Diaz de la Rubia, T. (2001). Parameter-Free Modelling of Dislocation Motion: The Case of Silicon, *Phil. Mag*., Vol. 81, No. 5, pp. 1257-1281

Bulatov, V.V. & Cai, W. (2006). *Computer Simulations of Dislocations*, Oxford Univ. Press, Oxford

Burgers, W.G. & Burgers, J.M. (1935). First report on viscosity and plasticity. *Kon. Nederl. Akad. v. Wet., Sect. 1,* Vol. 15, No. 3

Burgers, J.M. (1939). Some Considerations on the Fields of Stress Connected with Dislocations in a Regular Crystal Lattice. *Kon. Nederl. Akad. v. Wet.* Vol. 42, pp. 293-325

Burgers, J.M. (1940). Geometrical Considerations Concerning the Structural Irregularities to be Assumed in a Crystal, *Proc. Phys. Soc. London,* Vol. 52, pp. 23-33

Chadwick, G.A. & Smith, D.A. (1976). *Grain Boundary Structure and Properties*, Academic Press, London

Chelikowsky, J.R. (1982). 30° Partial Dislocations in Silicon: Absence of Electrically Active States, *Phys. Rev. Lett*., Vol. 49, No. 21, pp. 1569-1572

Chen, J., Yang, D., Xi, Z., and Sekiguchi, T. (2005). Electron-Beam-Induced Current Study of Hydrogen Passivation on Grain Boundaries in Multicrystalline Silicon: Influence of GB Character and Impurity Contamination, *Physica* B, Vol. 364, No. 1, pp. 162-169

Chen, J., Chen, B., Lee, W., Fukuzawa, M., Yamada, M., and Sekiguchi, T. (2010). Grain Boundaries in Multicrystalline Si, *Solid State Phenom*., Vol. 156-158, pp. 19-26

Cockayne, D.J.H., Ray, I.L.F. and Whelan, M.J. (1969). Investigations of Dislocation Strain Fields Using Weak Beams, *Phil. Mag*. Vol. 20, pp. 1265-1270

Corcoran, Y.L. & King, A.H. (1990). Grain Boundary Diffusion and Growth of Titanium Silicide Layers on Silicon, *J. Electron. Mat*., Vol. 19, No. 11, pp. 11771183

Cottrell, A.H. (1953). *Dislocations and Plastic Flow in Crystals*, Clarendon, Oxford

Csányi, G., Engeness, T.D., Ismail-Beigi, S., and Arias, T.A. (2000). New Physics of the 30° Partial Dislocation in Silicon Revealed Through ab initio Calculations, *J. Phys.: Condens. Mater*. Vol. 12, pp. 10029-10037

Dehlinger, U. & Kochendörfer, A. (1940). Eigenbewegungen in Kristallgittern. *Z. Phys.* Vol. 116, pp. 576-585

Donolato, C. (1979). Contrast and Resolution of SEM Charge-Collection Images of Dislocations, *Appl. Phys. Lett*., Vol. 34, No. 1, pp. 80-81

Donolato, C. (1983). Quantitative Evaluation of the EBIC Contrast of Dislocations, *J. Physique Coll*., Vol. 44, No. 9, pp. C4-269 – 275

Dreckschmidt, F. & Möller, H.-J. (2011). Defect Luminescence at Grain Boundaries in Multicrystalline Silicon, *Phys. Stat. Sol.* (c) Vol. 8, No. 4, pp. 1356-1360

Drozdov, N.A., Patrin, A.A., and Tkachev, V.D. (1976). Recombination Radiation on Dislocations in Silicon, *Pisma Zh. Eksp. Teor. Fiz*., Vol. 23, No. 11, pp. 651-653, *Sov. Phys. JETP Lett*. Vol. 23, pp. 597-599

Drozdov, N.A., Patrin, A.A., and Tkachev, V.D., On the Nature of the Dislocation Luminescence in Silicon, *Phys. Stat. Sol.* (b), Vol. 83, No. 2, pp. K137-K139

Duesbery, M.S. & Richardson, G.Y. (1991). The Dislocation Core in Crystalline Materials, *Rev. Solid State Mater. Sci*. Vol 17, No. 1, pp. 1-46

Duesbery, M.S., Joos, B., and Michel, D.J. (1991). Dislocation Core Studies in Empirical Silicon Models, *Phys. Rev*. B, Vol. 43, No. 6, pp. 5143-5146

Duesbery, M.S. & Joós, B. (1996). Dislocation Motion in Silicon: The Shuffle-Glide Controversy, *Phil Mag. Lett*., Vol. 74, No. 4, pp. 253-258

Eshelby, J.D. (1949). Edge Dislocations in Anisotropic Materials. *Phil. Mag*. Vol. 7, No. 40, pp. 903-912

Figielski, T. (1990). Electron Emission from Extended Defects: DLTS Signal in Case of Dislocation Traps, *Phys. Stat. Sol.* (a), Vol. 121, No. 1, pp. 187-193

Fossum, J.G. & Sundaresan, R. (1982). Analysis of Minority-Carrier Transport in Polysilicon Devices, *IEEE Trans. Electron. Dev*., Vol. ED-29, No. 8, pp. 1185-1197

Frank, F.C. (1951). Crystal Dislocations – Elementary Concepts and Definitions, *Phil. Mag*. Vol. 42, No. 331, pp. 809-819

Friedel, J. (1979). Dislocations – an Introduction, in: *Dislocation in Solids*, Vol. 1, F.R.N. Nabarro, pp. 1-32, North-Holland, Amsterdam

Gallagher, C.J. (1952). Plastic Deformation of Germanium and Silicon, *Phys. Rev*. Vol. 88, No. 4, pp. 721-722

George, A. & Yip, S. (2001).Preface to the Viewpoint Set on: Dislocation Mobility in Silicon, *Scripta Mat*., Vol. 45, pp. 1233-1238

Gleiter, H. & Chalmers, B. (1972). *High-Angle Grain Boundaries*, Pergamon Press, Oxford

Gomez, A., Cockayne, D.J.H., Hirsch, P.B., and Vitek, V. (1974). Dissociation of Near-Screw Dislocations in Germanium and Silicon, *Phil. Mag*. Vol. 31, pp. 105-113

Gomze, A.M. & Hirsch, P.B. (1977). On the Mobility of Dislocations in Germanium and Silicon, *Phil. Mag*. Vol. 36, No.1, pp. 169-179

Gundel, P. Schubert, M.C., Kwapil, W., Schön, J., Reiche, M., Savin, H., Yli-Koski, M., Sans, J.A., Martinez-Criado, G., Seifert, W., Warta, W., and Weber, E.R. (2009). Micro-Photoluminescence Spectroscopy on Metal Precipitates in Silicon, *Phys. Stat. Sol. RRL*, pp. 1-3

Gundel, P., Schubert, M.C., Heinz, F.D., Kwapil, W., Warta, W., Martinez-Criado, G., Reiche, M., and Weber, E.R. (2010). Impact of Stress on the Recombination at Metal Precipitates in Silicon, *J. Appl. Phys*. 108, pp. 103707-1 - 5

Heggie, M. & Jones, R. (1982). Glide of Partial Dislocations in Silicon, *J. Physique, Coll*., Vol. 43, No. 10, pp. 45-50

Heggie, M. & Jones R. (1983). Solitons and the Electrical and Mobility Properties of Dislocations in Silicon, *Phil. Mag*., Vol. 48, No. 4, pp. 365-377

Heggie, M.I., Jones, R., and Umerski, A. (1993). Ab Initio Energy Calculations of Impurity Pinning in Silicon, *Phys. Stat. Sol.* (a), Vol. 138, pp. 383-387

Higgs, V., Lightowlers, E.C., Fitzgerald, E.A., Xie, Y.H., and Silverman, P.J. (1993). Characterization of Compositionally Graded $Si_{1-x}Ge_x$ Alloy Layers by Photoluminescence Spectroscopy and by Cathodoluminescence Spectroscopy and Imaging, *J. Appl. Phys*., Vol. 73, No. 4, pp. 1952-1956

Hirsch, P.B. (1979). Recent Results on the Structure of Dislocations in Tetrahedrally Coordinated Semiconductors, *J. Physique, Coll*., Vol. 40, No. 6, pp. C6-27 - 32

Hirsch, P.B. (1985). Dislocations in Semiconductors, *Mat. Sci. Technol*., Vol. 1, No. 9, pp. 666-677

Hirth, J.P. & Lothe, J. (1982). *Theory of Dislocations*, Wiley Interscience, New York

Hornstra, J. (1958). Dislocations in the Diamond Lattice, *J. Phys. Chem. Solids*, Vol. 5, pp. 129-141

Ishikawa, Y., Yamamoto, C., and Tabe, M. (2006). Single-Electron Tunneling in a Silicon-On-Insulator Layer Embedding an Artificial Dislocation Network, *Appl. Phys. Lett.*, Vol. 88, pp. 073112-1 - 3

Jones, R., Umerski, A., Stich, P., Heggie, M.I., and Öberg, S. (1993). Density Functional Calculations of the Structure and Properties of Impurities and Dislocations in Semiconductors, *Phys. Stat. Sol.* (a), Vol. 138, pp. 369-381

Jones, R., Coomer, B.J., Goss, J.P., Öberg, S., and Briddon, P.R. (2000). Intrinsic Defects and the D1 to D4 Optical Bands Detected in Plastically Deformed Si, *Phys. Stat. Sol.* (b), Vol. 222, No. 1, pp. 133-140

Joshi, D.P. (1987). Grain Boundary Recombination in Polycrystalline Silicon Under Optical Illumination, *Phys. Stat. Sol.* (a), Vol. 108, No. 2, pp. 213-218

Kisielowski-Kemmerich, C. (1990). Vacancies and Their Complexes in the Core of Screw Dislocations: Models which Account for ESR Investigations of Deformed Silicon, *Phys. Stat. Sol.* (b), Vol. 161, pp. 11-42

Keyes, R.W. (1960). The Effects of Elastic Deformation on the Electrical Conductivity of Semiconductors, *Solid State Phys.*, Vol. 11, pp. 149-221

Kittler, M., Yu, X., Mchedlidze, T., Arguirov, T., Vyvenko, O.F., Seifert, W., Reiche, M., Wilhelm, T., Seibt, M., Voß, O., Wolff, A., and Fritzsche, W. (2007). Regular Dislocation Networks in Silicon as a Tool for Nanostructure Devices Used in Optics, Biology, and Electronics, *Small*, Vol. 3, No. 6, pp. 964-973

Kittler, M. & Reiche, M. (2009). Dislocations as Active Components in Novel Silicon Devices, *Adv. Eng. Mater.* Vol. 11, No. 4, 249-258

Kochendörfer, A. (1938). Theorie der Kristallplastizität, *Z. Phys.* Vol. 108, No. 3-4, pp. 244-264

Kveder, V., Kittler, M., and Schröter, W. (2001). Recombination Activity of Contaminated Dislocations in Silicon: A Model Describing Electron-Beam-Induced Current Contrast Behavior, *Phys. Rev.* B, Vol. 63, pp. 115208-1 - 11

Kveder, V. & Kittler, M. (2008). Dislocations in Silicon and D-Band Luminescence for Infrared Light Emitters, *Mat. Sci. Forum*, Vol. 590, pp. 29-56

Labusch, R. & Schröter, W. (1980). Electrical Properties of Dislocations in Semiconductors, in: *Dislocation in Solids*, Vol. 5, F.R.N. Nabarro, pp. 127-191, North-Holland, Amsterdam

Lang, D.V. (1974). Deep-Level Transient Spectroscopy: A New Method to Characterize Traps in Semiconductors, *J. Appl. Phys.*, Vol. 45, No. 7, pp. 3023-3032

Lee, W., Chen, J., Chen, B., Chang, J., and Sekiguchi, T. (2009). Cathodoluminescence Study of Dislocation-Related Luminescence From Small-Angle Grain Boundaries in Multicrystalline Silicon, *Appl. Phys. Lett.*, Vol. 94, pp. 112103-1 - 3

Lehto, N. & Öberg, S. (1998) Effects of Dislocation Interactions: Application to the Period-Double Core of the 90° Partial in Silicon, *Phys. Rev. Lett.*, Vol. 80, No. 25, pp. 5568-5571

Li, C., Meng, Q., Zhong, K., and Wang, C. (2008). Computer Simulation of the 60° Dislocation Interaction with Vacancy Cluster in Silicon, *Phys. Rev.* B, Vol. 77, pp. 045211-1 – 045211-5

Lodge, K.W., Lapiccirella, A., Battistoni, C., Tomassini, N., and Altmann, S.L. (1989). The 90° Partial Dislocation in Silicon: Geometry and Electronic Structure, *Phil. Mag*. A, Vol. 60, No. 5, pp. 643-651

Love, A.E.H. (1927). *A Treatise on the Mathematical Theory of Elasticity*, Cambridge University Press, Cambridge, p. 221

Marklund, S. (1979). Electron States Associated with Partial Dislocations in Silicon, *Phys. Stat. Sol*. (b), Vol. 92, pp. 83-89

Marklund, S. (1981). Energy Levels of Intrinsic and Extrinsic Stacking Faults in Silicon, *Phys. Stat. Sol*. (b), Vol. 108, pp. 97-102

Marklund, S. (1983). Structure and Energy Levels of Dislocations in Silicon, *J. Physique, Coll*., Vol 44, No. 9, C4-25 - 35

Mataré, H.F. (1984). Carrier Transport at Grain Boundaries in Semiconductors, *J. Appl. Phys*., Vol. 56, No. 10, pp. 2605-2631

Mattheiss, L.F. & Patel, J.R. (1981). Electronic Stacking Fault States in Silicon, *Phys. Rev*. B, Vol. 23, No. 10, 5384-5396

Mchedlidze, T., Arguirov, T., Kouteva-Argoirova, S., and Kittler, M. (2010). Characterization of Thin Film Photovoltaic Material Using Photoluminescence and Raman Spectroscopy, *Solid-State Phenom*. Vol. 156-158, pp. 419-424

Milshtein, S. (1979). Application of Dislocation-Induced Potentials in Si and Ge, *J. Physique, Coll*., Vol. 40, No. 6, pp. C6-207 - 211

Mueller, R.K. (1961). Current Flow Across Grain Boundaries in n-Type Germanium I, *J. Appl. Phys*., Vol. 32, No. 4, pp. 635-639

Nabarro, F.R.N. (1947). Dislocations in a Simple Cubic Lattice. *Proc. Phys. Soc. London*, Vol. 59, pp. 256-272

Northrup, J.E., Cohen, M.L., Chelikowsky, J.R., Spence, J., and Olsen, A. (1981). Electronic Structure of the Unreconstructed 30° Partial Dislocation in Silicon, *Phys. Rev*. B, Vol. 24, No. 8, pp. 4623-4628

Orowan, E. (1934). Zur Kristallplastizität III. *Z. Phys*. Vol. 89, pp. 634-659

Pandelov, S., Seifert, W., Kittler, M., and Reif, J. (2002). Analysis of Local Electrical Properties of Grain Boundaries in Si by Electron-Beam-Induced-Current Techniques, *J. Phys.: Condens. Matter*, Vol. 14, pp. 13161-13168

Pasemann, L. (1981). A Contribution to the Theory of the EBIC Contrast of Lattice Defects in Semiconductors, *Ultramicroscopy*, Vol. 6, pp. 237-250

Pearson, G.L., Read, W.T., and Morin, F.J. (1954). Dislocations in Plastically Deformed Germanium. *Phys. Rev*. Vol. 93, No. 4, pp. 666-667

Peierls, R. (1940). The Size of a Dislocation. *Proc. Phys. Soc. London*, Vol. 52, pp. 34-37

Polanyi, M. (1934). Über eine Art Gitterstörung, die einen Kristall plastisch machen könnte. *Z. Phys*. Vol. 89, pp. 660-664

Queisser, H.J., Hubner, K., and Shockley, W. (1961). Diffusion Along Small-Angle Grain Boundaries in Silicon, *Phys. Rev*. Vol. 123, No. 4, pp. 1245-1254

Ray, I.L.F. & Cockayne, D.J.H. (1971). The Dissociation of Dislocations in Silicon, *Proc. R. Soc. London*, A, Vol. 325, pp. 543-554

Read, W.T. (1954a). Theory of Dislocations in Germanium, *Phil. Mag*. Vol. 45, No. 367, pp. 775-796

Read, W.T. (1954b). Statistics of the Occupation of Dislocation Acceptor Centres, *Phil. Mag*. Vol. 45, No. 370, pp. 1119-1128

Read, W.T. & Shockley, W. (1950). Dislocation Models of Crystal Grain Boundaries, *Phys. Rev*., Vol. 78, No. 3, pp. 275-289

Reiche, M. (2008). Dislocation Networks Formed by Silicon Wafer Direct Bonding, *Mater. Sci. Forum*, Vol. 590, pp. 57-78

Reiche, M., Kittler, M., Buca, D., Hähnel, A., Zhao, Q.-T., Mantl, S., and Gösele, U. (2010). Dislocation-Based Si-Nanodevices, *Jpn. J. Appl. Phys*., Vol. 49, pp. 04DJ02-1 - 5

Reiche, M., Kittler, M., Scholz, R., Hähnel, A., and Arguirov, T. (2011). Structure and Properties of Dislocations in Interfaces of Bonded Silicon Wafers, *J. Phys. Conf. Ser*., Vol. 281, pp. 012017-1 - 10

Rinio, M., Kaes, M., Hahn, G., and Borchert, D. (2006). Hydrogen Passivation of Extended Defects in Multicrystalline Silicon Solar Cells, *Proc. 21st Europ. Photovolt. Solar Energy Conf*., Dresden

Salman, F., Arnold, J., Zhang, P., Chai, G., Stevie, F.A., and Chow, L. (2007). Redistribution of Implanted Species in Polycrystalline Silicon Films on Silicon Substrate, *Defect & Diff. Forum*, Vol. 264, pp. 7-12

Sauer, R., Weber, J., Stolz, J., Weber, E.R., Küsters, K.-H., and Alexander, H. (1985). Dislocation-Related Photoluminescence in Silicon, *Appl. Phys. A*, Vol. 36, No. 1, pp. 1-13

Schimpf, K., Palm, J., and Alexander, H. (1994). Enhanced Diffusion of Phosphorous at Grain Boundaries in Multicrystalline Silicon, *Cryst. Res. Technol*. Vol. 29, No. 8, pp. 1123-1129

Schmid, R.P., Mankovics, D., Arguirov, T., Mchedlidze, T., and Kittler, M. (2011). Novel Imaging Techniques for Dislocation-Related D1-Photoluminescence of Multicrystalline Si Wafers – Two Different Approaches, *Phys. Stat. Sol. (c)*, Vol. 8, No. 4, pp. 1297-1301

Schröter, W. (1969). Trägerbeweglichkeit in verformtem Germanium, *Phys. Stat. Sol*., Vol. 31, No. 1, pp. 177-186

Schröter, W. & Labusch, R. (1969). Electrical Properties of Dislocations in Ge and Si. *Phys. Stat. Sol.* Vol. 36, pp. 539-550

Schröter, W. & Cerva, H. (2002). Interaction of Point Defects with Dislocations in Silicon and Germanium: Electrical and Optical Effects, *Solid State Phenom*. Vol. 85-86, pp. 67-144

Seager, C.H. (1985). Grain Boundaries in Polycrystalline Silicon, *Ann. Rev. Mater. Sci*., Vol. 15, pp. 271-302

Seager, C.H. & Pike, G.E. (1979). Grain Boundary States and Varistor Behavior in Silicon Bicrystals, *Appl. Phys. Lett*., Vol. 35, No. 9, pp. 709-711

Seibt, M., Khalil, R., Kveder, V., and Schröter, W. (2009a). Electronic States at Dislocations and Metal Silicide Precipitates in Crystalline Silicon and Their Role in Solar Cell Materials, *Appl. Phys*. A, Vol. 96, pp. 235-253

Seibt, M., Abdelbarey, D., Kveder, V., Rudolf, C., Saring, P., Stolze, L., and Voß, O. (2009b). Structure, Chemistry and Electrical Properties of Extended Defects in Crystalline Silicon for Photovoltaics, *Phys. Stat. Sol*. (c), Vol. 6, No. 8, pp. 1847-1855

Seitz, F. (1952). The Plasticity of Silicon and Germanium, *Phys. Rev*. Vol. 88, No. 4, pp. 722-724

Sekiguchi, T., Chen, J., Lee, W., and Onodera, H. (2011). Electrical and Optical Activities of Small Angle Grain Boundaries in Multicrystalline Si, *Phys. Stat. Sol*. (c), Vol. 8, No. 4, pp. 1347-1350

Shikin, V.B. & Shikina, Y.V. (1995). Charged Dislocations in Semiconductor Crystals, *Usp. Fiz. Nauk*, Vol. 165, No. 8, pp. 887-917, *Physics-Uspekhi*, Vol. 38, No. 8, pp. 845-875

Shockley, W. (1953). Dislocations and Edge States in the Diamond Crystal Structure, *Phys. Rev*., Vol. 91, p. 228

Shockley, W. & Read, W.T. (1949). Quantitative Predictions from Dislocation Models of Crystal Grain Boundaries, *Phys. Rev*., Vol. 75, p. 692

Spence, J.C.H. (2007). Experimental studies of Dislocation Core Defects, in: *Dislocation in Solids*, Vol. 13, F.R.N. Nabarro and J.P. Hirth, pp. 419-452, Elsevier, Amsterdam

Sutton, A. & Baluffi, R.W. (1995). *Interfaces in Crystalline Materials*, Oxford University Press, Oxford

Taylor, G.I. (1934a). The Mechanism of Plastic Deformation of Crystals. Part I.-Theoretical. *Proc. R. Soc. London*, Vol. 145, No. 855, pp. 362-387

Taylor, G.I. (1934b). The Mechanism of Plastic Deformation of Crystals. Part II. - Comparison with Observations. *Proc. R. Soc. London*, Vol. 145, No. 855, pp. 388-404

Taylor, W.E., Odell, N.H., and Fan, H.Y. (1952). Grain Boundary Barriers in Germanium, *Phys. Rev*., Vol. 88, No. 4, pp. 867-875

Thibault-Desseaux, J., Putaux, J.L., Bourret, A., and Kirchner, H.O.K. (1989). Dislocations Stopped by the $\Sigma = 9(122)$ Grain Boundary in Si. An HREM Study of Thermal Activation, *J. Physique*, Vol. 50, pp. 2525-2540

Tong, Q.Y. & Gösele, U. (1998). *Semiconductor Wafer Bonding. Science and Technology*, Wiley, New York

Van der Merwe, J.H. (1950), On the Stress and Energies Associated with Inter-Crystalline Boundaries, *Proc. Phys. Soc. London*, A Vol. 63, pp. 616-637

Vernon-Parry, K.D., Davies, G., and Galloway, S. (2005). Electronic and Structural Properties of Grain Boundaries in Electron-Irradiated Edge-Defined Film-Fed Growth Silicon, *Semicond. Sci. Technol*., Vol. 20, pp. 171-174

Veth, H. & Lannoo, M. (1984). The Electronic Properties of Charged Dislocations in Semiconductors, *Phil. Mag*. B, Vol. 50, No. 1, pp. 93-102

Volterra, V. (1907). Sur l`équilibre des corps élastiques multiplement connexes, *Ann. Sci. Ecole Norm. Super*., Vol. 24, No. 3, pp. 401-517

Watson, G.P., Benton, J.L., Xie, Y.H., and Fitzgerald, E.A. (1998). Influence of Misfit Dislocation Interactions on Photoluminescence Spectra of SiGe on Patterned Si, *J. Appl. Phys*., Vol. 83, No. 7, pp. 3773-3776

Weber, H., Schröter, W., and Haasen, P. (1968). Elektronenzustände an Versetzungen in Silizium, *Helv. Phys. Acta*, Vol. 41, pp. 1255-1258

Weber, J. & Alonso, M.I. (1990). Detection of Dislocation-Related Photoluminescence Bands in Si-Ge Alloys Grown by Liquid Phase Epitaxy, in: *Defect Control in Semiconductors*, K. Sumino, Vol. 2, pp. 1453-1457, North-Holland, Amsterdam

Weber, J. (1994). Correlation of Structural and Electronic Properties from Dislocations in Semiconductors, *Solid State Phenom.*, Vol. 37-38, pp. 13-24

Wilhelm, T, Mchedlidze, T., Yu, X., Arguirov, T., Kittler, M. and Reiche, M. (2008). Regular Dislocation Networks in Silicon. Part I: *Structure, Solid State Phenom*., Vol. 131-133, pp. 571-578

Wilshaw, P.R. & Booker, G.R. (1985). New Results and an Interpretation for SEM EBIC Contrast Arising from Individual Dislocations in Silicon., *Inst. Phys. Conf. Ser*., Vol. 76, pp. 329-336

Würfel, P. (1982). The Chemical Potential of Radiation, *J. Phys. C: Solid State Phys*., Vol. 15, pp. 3967-3985

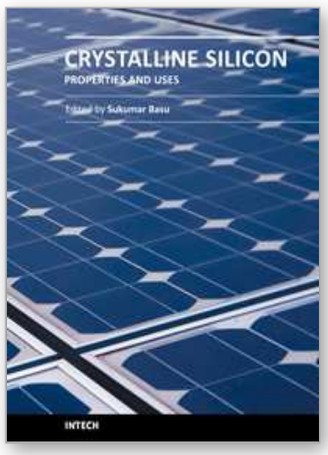

Crystalline Silicon - Properties and Uses
Edited by Prof. Sukumar Basu

ISBN 978-953-307-587-7
Hard cover, 344 pages
Publisher InTech
Published online 27, July, 2011
Published in print edition July, 2011

The exciting world of crystalline silicon is the source of the spectacular advancement of discrete electronic devices and solar cells. The exploitation of ever changing properties of crystalline silicon with dimensional transformation may indicate more innovative silicon based technologies in near future. For example, the discovery of nanocrystalline silicon has largely overcome the obstacles of using silicon as optoelectronic material. The further research and development is necessary to find out the treasures hidden within this material. The book presents different forms of silicon material, their preparation and properties. The modern techniques to study the surface and interface defect states, dislocations, and so on, in different crystalline forms have been highlighted in this book. This book presents basic and applied aspects of different crystalline forms of silicon in wide range of information from materials to devices.

How to reference
In order to correctly reference this scholarly work, feel free to copy and paste the following:

Martin Kittler and Manfred Reiche (2011). Structure and Properties of Dislocations in Silicon, Crystalline Silicon - Properties and Uses, Prof. Sukumar Basu (Ed.), ISBN: 978-953-307-587-7, InTech, Available from: http://www.intechopen.com/books/crystalline-silicon-properties-and-uses/structure-and-properties-of-dislocations-in-silicon

INTECH
open science | open minds

InTech Europe
University Campus STeP Ri
Slavka Krautzeka 83/A
51000 Rijeka, Croatia
Phone: +385 (51) 770 447
Fax: +385 (51) 686 166
www.intechopen.com

InTech China
Unit 405, Office Block, Hotel Equatorial Shanghai
No.65, Yan An Road (West), Shanghai, 200040, China
中国上海市延安西路65号上海国际贵都大饭店办公楼405单元
Phone: +86-21-62489820
Fax: +86-21-62489821

IntechOpen